A unified image registration framework for ITK

Members of ITK community

No Institute Given

Abstract. Publicly available scientific resources help establish evaluation standards, provide a platform for teaching and may improve reproducibility. Version 4 of the Insight ToolKit (ITK[4]) seeks to establish new standards in publicly available image registration methodology. In this work, we provide an overview and preliminary evaluation of the revised toolkit against registration based on the previous major ITK version (3.20). Furthermore, we propose a nomenclature that may be used to discuss registration frameworks via schematic representations. In total, the ITK[4] contribution is intended as a structure to support reproducible research practices, will provide a more extensive foundation against which to evaluate new work in image registration and also enable application level programmers a broad suite of tools on which to build.

1 Introduction

As image registration methods mature—and their capabilities become more widely recognized—the number of applications increase [20, 22, 21, 16, 5, 6, 3, 19, 15, 13, 8, 17]. Consequently, image registration transitioned from being a field of active research, and few applied results, to a field where the main focus is translational. Image registration is now used to derive quantitative biomarkers from images [11], plays a major role in business models and clinical products (especially in radiation oncology) [6], has led to numerous new findings in studies of brain and behavior (e.g. [4]) and is a critical component in applications in pathology, microscopy, surgical planning and more [21, 16, 9, 5, 6, 19, 13, 17]. Despite the increasing relevance of image registration across application domains, there are relatively few reference algorithm implementations available to the community.

One source of benchmark methodology is the Insight ToolKit (ITK) [24, 1], which marked a significant contribution to medical image processing when it first emerged over 10 years ago. Since that time, ITK has become a standard-bearer for image processing algorithms and, in particular, for image registration methods. In a review of ITK user interests, image registration was cited as the most important contribution of ITK (personal communication). Numerous papers use ITK algorithms as standard references for implementations of Demons registration and mutual information-based affine or B-Spline registration [22, 21, 9, 5, 6]. Multiple toolkits extend ITK registration methods in unique ways. Elastix provides very fast and accurate B-Spline registration [14, 17]. The diffeomorphic demons is a fast/efficient approximation to a diffeomorphic mapping [23]. ANTs provides both flexibility and high average performance [2]. The BrainsFit algorithm is integrated into slicer for user-guided registration [13]. Each of these toolkits has both strengths and weaknesses [14, 17] and was enabled by an ITK core.

The Insight ToolKit began a major refactoring effort in 2010. The refactoring aimed to both simplify and extend the techniques available in version 3.x with methods and ideas from a new set of prior work [12, 7, 20, 16, 19, 2]. To make this technology more accessible, ITK[4] unifies the dense registration framework (displacement field, diffeomorphisms) with the low-dimensional (B-Spline, Affine, rigid) framework by introducing composite transforms, deformation field transforms and specializations that allowed these to be optimized efficiently. A sub-goal set for ITK[4] was to simplify parameter setting by adding helper methods that use well-known principles of image registration to automatically scale transform components and set optimization parameters. ITK[4] transforms are also newly applicable to objects such as vectors and tensors and will take into account covariant geometry if necessary. Finally, ITK[4] reconfigures the registration framework to use multi-threading in as many locations as possible. The revised registration framework within ITK is more thoroughly integrated across transform models, is thread-safe and provides broader functionality than in prior releases.

The remainder of the document will provide an overview of the new framework via the context of a potential general nomenclature. We also establish performance benchmarks for the current ITK[4] registration. Finally, we discuss future developments in the framework.

2 Nomenclature

The nomenclature below designates an image registration algorithm pictorially. This nomenclature is intended to be a descriptive, but also technically consistent, system for visually representing algorithms and applications of registration. Ideally, any standard algorithm can be written in the nomenclature below.

A physical point: $x \in \Omega$ where Ω is the domain, usually of an image.

An image: $I \colon \Omega^d \to \mathbb{R}^n$ where n is the number of components per pixel and d is dimensionality. A second image is J.

Domain map: $\phi \colon \Omega_I \to \Omega_J$ where $\to$ may be replaced with any mapping symbol below.

Affine mapping: $\leftrightarrow$ a low-dimensional invertible transformation: affine, rigid, translation, etc.

Affine mapping: $\to$ designates the direction an affine mapping is applied.

Deformation field: $\rightsquigarrow$ deformation field mapping J to I. May not be invertible.

Spline-based mapping: $\overset{\rightsquigarrow}{b}$ e.g. B-Spline field mapping J to I.

Diffeomorphic mapping: $\leftrightsquigarrow$ these maps should have an accurate inverse that is computed in the algorithm or can be computed from the results.

Composite mapping: $\phi = \phi_1(\phi_2(x))$ is defined by $\leftrightsquigarrow\to$ where ϕ_2 is of type $\leftrightsquigarrow$.

Not invertible: $\leftrightarrow\!\!\!/$ indicates a mapping that is not guaranteed invertible.

Similarity measure: $\overset{\approx}{s}$ or $\approx_s$ indicates that statistical measure s is used to compare images.

We would then write a standard Demons registration application that maps one image, J, into the space of I (presumably a template) as:

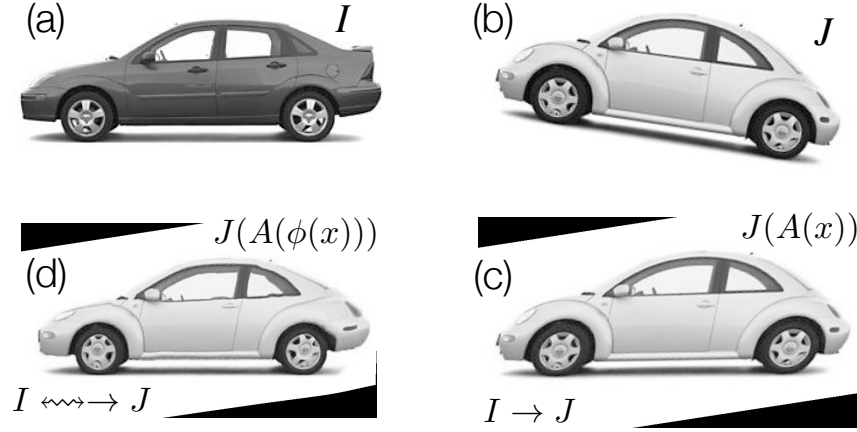$$I \rightsquigarrow\to J \quad \text{which symbolizes} \quad I \approx J(A(\phi(x))),$$

Fig. 1. The standard approach in the ITKv4 registration framework is to map image J (b) to image I (a) by first identifying the linear transformation that removes (a sub-space of) affine variation between the images as in (c). Second, we remove the shape (diffeomorphic) differences (d). This results in a composite mapping, computed via the mutual information similarity metric, that identifies $I(x) \approx_{\mathrm{mi}} J(A(\phi(x))) = J_{\mathrm{Affine}}(y) = J(z)$. The image $J_{\mathrm{Affine}}(y)$ represents J after application of the affine transformation A i.e. $J(A(x))$.

with A an affine mapping and ϕ a generic deformation. The notation means that the algorithm first optimizes an affine mapping, $\to$, between J and I. This is followed by a deformation. We denote the similarity metric as $\approx$ which indicates a sum of squared differences (the default similarity metric). ITK^4 supports metrics such as mutual information, $\underset{\mathrm{mi}}{\approx}$, or cross-correlation, $\underset{\mathrm{cc}}{\approx}$. The second stage computes a deformation, $\rightsquigarrow$, from $\to J$ to I. In terms of transformation composition, we would write $\rightsquigarrow\to J = J_w(x) = J(\phi_{\mathrm{Affine}}(\phi_{\mathrm{Demons}}(x)))$ where J_w is the result of warping J to I. The ϕ are the specific functions corresponding to the schematic arrows. Note, also, that the tail of the arrow indicates the transform's domain. The arrowhead indicates its range. We will use this nomenclature to write schematics for registration applications in the following sections.

3 Overview of the unified framework

The key ideas for ITK^4 registration are:

1. Registration maps can be applied or optimized through the *itkCompositeTransform* which chains transforms together as in Figure 1.
2. Each transform has either global support (affine transform) or local support (a displacement field transform). If any map in a composite transform has global support then the composite transform has global support.

3. ITK^4 metrics are applicable to both types of transforms and may optimize over dense or sparse samples from Ω. Metrics may be multi-channel (e.g. for registering RGB or tensor images).

4. The optimization framework is multi-threaded and memory efficient to allow high-dimensional transformations to be optimized quickly on multi-core systems.

5. The ITK^4 optimization framework comes with parameter setting tools that automatically select parameter scales and learning rates for gradient-based optimization schemes. These parameter setting tools use physical units to help provide the user with intuition on the meaning of parameters.

Below we will discuss (1) gradient-based optimization within the framework, (2) techniques to estimate optimization parameters for arbitrary metric and transformation combinations and (3) a generalized diffeomorphic matching approach.

3.1 Optimization Framework

The general ITK^4 optimization criterion is summarized as:

$$\text{Find mapping } \phi(x, p) \in \mathcal{T} \text{ such that } M(I, J, \phi(x, p)) \text{ is minimized.} \tag{1}$$

While, for functional mappings, this formulation is not strictly correct, the practical implementation of even high-dimensional continuous transformations involves parameterization. The space $\mathcal{T}$ restricts the possible transformations over which to optimize the mapping ϕ. The arguments to ϕ are its parameters, p, and the spatial position, x. Note that, in ITK^4, the image I may also contain a mapping, although it is not directly optimized in most cases. As will be seen later in the document, this mapping may also be used within large deformation metrics.

The similarity metric, M, is perhaps the most critical component in image registration. Denote a parameter set as $p = (p_1, p_2 \ldots p_n)$. The metric (or comparison function between images) is then defined completely as $M(I, J, \phi(x, p))$. For instance, $M = \|I(x) - J(\phi(x, p))\|^2$ i.e. the sum of squared differences (SSD) metric. Its gradient with respect to parameter p_i is (using the chain rule),

$$M_{p_i} = \frac{\partial M}{\partial p_i} = \frac{\partial M}{\partial J} \frac{\partial J(\phi(x, p))}{\partial \phi} \frac{\partial \phi}{\partial p_i} |_x \quad . \tag{2}$$

This equation provides the metric gradient specified for sum of squared differences (at point x) but similar forms arise for the correlation and mutual information [10]. Both are implemented in ITK^4 for transformations with local and global support. The $\frac{\partial J(\phi(x,p))}{\partial \phi}$ term is the gradient of J at $\phi(x)$ and $\frac{\partial \phi}{\partial p_i}$ is the Jacobian of the transformation taken with respect to its parameter. The transform $\phi(x, p)$ may be an affine map i.e. $\phi(x, p) = Ax + t$ where A is a matrix and t a translation. Alternatively, it may be a displacement field where $\phi(x, p) = x + u(x)$ and u is a vector field. In ITK^4, both types of maps are interchangeable and may be used in a composite transform to compute registrations that map to a template via a schematic such as $I \approx\to J$, $I \underset{\text{mi}}{\overset{\approx}{\to}} \overset{\rightharpoonup}{b} \to J$, $I \overset{\approx}{\underset{\text{cc}}{\to}} \leftrightsquigarrow\to J$ or, mixing similarity metrics, $I \underset{\text{cc}}{\approx} \leftrightsquigarrow \underset{\text{mi}}{\approx} \to J_i$.

The most commonly used optimization algorithm for image registration is gradient descent, or some variant. In the above framework, the gradient descent takes on the form of

$$\phi(p_{\text{new}}, x) = \phi(p_{\text{old}} + \lambda \left[\frac{\partial M}{\partial p_1}, \cdots, \frac{\partial M}{\partial p_n} \right], x),$$

where λ is the overall learning rate and the brackets hold the vector of parameter updates. Note that, as in previous versions of ITK, a naive application of gradient descent will not produce a smooth change of parameters for transformations with mixed parameter types. For instance, a change Δ to parameter p_i will produce a different magnitude of impact on ϕ if p_i is a translation rather than a rotation. Thus, we develop an estimation framework that sets "parameter scales" (in ITK parlance) which, essentially, customize the learning rate for each parameter. As a footnote, the update to ϕ via its gradient may also include other steps (such as Gaussian smoothing) that project the updated transform back to space $\mathcal{T}$.

3.2 Parameter scale estimation

We choose to estimate parameter scales by analyzing the result of a small parameter update on the change in the magnitude of physical space deformation induced by the transformation. The impact from a unit change of parameter p_i may be defined in multiple ways, such as the maximum shift of voxels or the average norm of transform Jacobians [12].

Denote the unscaled gradient descent update to p as $\triangle p$. The goal is to rescale $\triangle p$ to $q = s \cdot \triangle p$, where s is a diagonal matrix $\text{diag}(s_1, s_2 \ldots s_n)$, such that a unit change of q_i will have the same impact on deformation for each parameter $i = 1...n$. As an example, we want $\|\phi(x, p_{\text{new}}) - \phi(x, p_{\text{old}})\| = constant$ regardless of which of the i parameters is updated by the unit change. The unit is an epsilon value, e.g. 1.e-3.

Rewrite $\left[\frac{\partial M}{\partial p_1}, \cdots, \frac{\partial M}{\partial p_n} \right]$ as $\frac{\partial M}{\partial J} \frac{\partial J(\phi(x,p))}{\partial \phi} \left[\frac{\partial \phi}{\partial p_1}, \cdots, \frac{\partial \phi}{\partial p_n} \right]$. To determine the relative scale effects of each parameter, p_i, we can factor out the constant terms on the outside of the bracket. Then the modified gradient descent step becomes $\text{diag}(s) \frac{\partial \phi}{\partial p}$. We identify the values of $\text{diag}(s)$ by explicitly computing the values of $\|\phi(x, p_{\text{new}}) - \phi(x, p_{\text{old}})\|$ with respect to an ϵ change. A critical variable, practically, is which x to choose for evaluation of $\|\phi(x, p_{\text{new}}) - \phi(x, p_{\text{old}})\|$. The corners of the image domain work well for affine transformations. In contrast, local regions of small radius (approximately 5) work well for transformations with local support. Additional work is needed to verify optimal parameters for this new ITK[4] feature. However, a preliminary evaluation is performed in the results section. The new parameter scale estimation effectively reduces the number of parameters that the user must tune from $k + 1$ (λ plus the scales for each parameter type where there are k types) to only 1, the learning rate.

The learning rate, itself, may not be intuitive for a user to set. The difficulty—across problem sets—is that a good learning rate for one problem may result in a different amount of change per iteration in another problem. Furthermore, the discrete image gradient may become invalid beyond one voxel. Thus, it is good practice to limit a deformation step to one voxel spacing [12]. We therefore provide the users the ability to specify the learning rate in terms of the *maximum physical space change per iteration*.
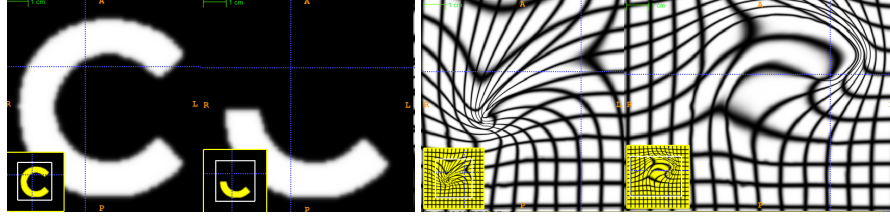
Fig. 2. An ITK diffeomorphic mapping of the type $I \leftrightsquigarrow J$. The "C" and 1/2 "C" example illustrate the large deformations that may be achieved with time varying velocity fields. In this case, the moving (deforming) image is the 1/2 "C". The right panels illustrate the deformed grid for the transformation of the "C" to 1/2 "C" (middle right) and its inverse mapping (far right) which takes the 1/2 "C" to the reference space. The unit time interval is discretized into 15 segments in order to compute this mapping. 15*5 integration steps were used in the Runge-Kutta *ode* integration over the velocity field. A two core MacBook Air computed this registration in 110 seconds. The images each were of size 150×150.

As with the parameter scale estimation, the domain over which this maximum change is estimated impacts the outcome and similar practices are recommended for both cases. This feature is especially useful for allowing one to tune gradient descent parameters without being concerned about which similarity metric is being used. That is, it effectively rescales the term $\lambda \partial M / \partial p$ to have a consistent effect, for a given λ, regardless of the metric choice.

3.3 Diffeomorphic mapping with arbitrary metrics

Beg proposed the Large Deformation Diffeomorphic Metric Mapping (LDDMM) algorithm [16] which minimizes the sum of squared differences criterion between two images. LDDMM parameterizes a diffeomorphism through a time varying velocity field that is integrated through an *ode*. In ITK[4] , we implement an alternative to LDDMM that also uses a time varying field and an *ode* but minimizes the following objective function:

$$E(\mathbf{v}) = M(I, J, \phi_{1,0}) + w \int_0^1 \|\mathcal{L}v_t\|^2 \mathrm{d}t \ . \tag{3}$$

This is an instance of equation 1 where w is a scalar weight and $\phi_{1,0}$ is a standard integration of the time-varying velocity field v_t which is regularized by linear operator $\mathcal{L}$. ITK[4] uses Gaussian smoothing which is the Green's kernel for generalized Tikhonov regularization [18]. This objective is readily optimized using an approach that is similar to that proposed by Beg. Generalization of the LDDMM gradient for other metrics basically follows [10] with a few adjustments to accomodate diffeomorphic mapping. Figure 2 shows an ITK result on a standard example for large deformation registration. We will evaluate this diffeomorphic mapping, along with parameter estimation, in the following section.

4 Evaluation

We first investigate the ability of our automated parameter estimation to facilitate parameter tuning across metrics. We then compare ITK[4] with an open-source ITK[3] registration application.

4.1 Parameter estimation across metrics

ITK[4] provides similarity metrics that may be applied for both deformable and affine registration. In a previous section, we provided a parameter estimation strategy that is applicable to both deformable and affine transformations with arbitrary metrics. Denote images I, J, K, where the latter two are "moving" images, and K is an intensity-inverted version of J. We then evaluate the following schema,

$$I \approx \leftsquigarrow \rightarrow J \tag{4}$$
$$I \approx_{\mathrm{cc}} \leftsquigarrow \rightarrow K$$
$$I \approx_{\mathrm{mi}} \leftsquigarrow \rightarrow K$$

where, for each schematic, we use the corresponding metric for both affine and diffeomorphic mapping. Furthermore, we keep the same parameters for each registration by exploiting our parameter scale estimators. Figure 3 shows the candidate images for this test.

As shown in figure 3, very similar results are achieved for each schematic with minimal parameter tuning. The sum of squared differences between the reference image I and the three target cases are 14.04, 191.6 and 184.0. The negative correlation between the reference image I and the three target cases are -0.650, -0.680 and -0.50. The mutual information between the reference image I and the three target cases are -1.132, -1.057 and -0.992. Thus, a single set of tuned parameters provides a reasonable result for an affine plus diffeomorphic mapping across three different metrics. While improvement might be gained by further tuning for each metric, this result shows that our parameter estimation method achieves the goal of reducing user burden.

4.2 Comparison against ITK[3]

We compare the ITK[4] registration against an ITK[3] registration suite BrainsFit (nitrc.org multimodereg). We present preliminary, encouraging evaluation results for this approach to gradient descent with both affine and deformable registration in Figure 4. The dataset consists of ten elderly and demented subjects with manual labels of brain parenchyma. Of importance is that the ventricles are not included in the parenchyma. Large deformation is required to match ventricles and, as such, this evaluation provides some insight into the benefit of the new ITK[4] diffeomorphic matching.
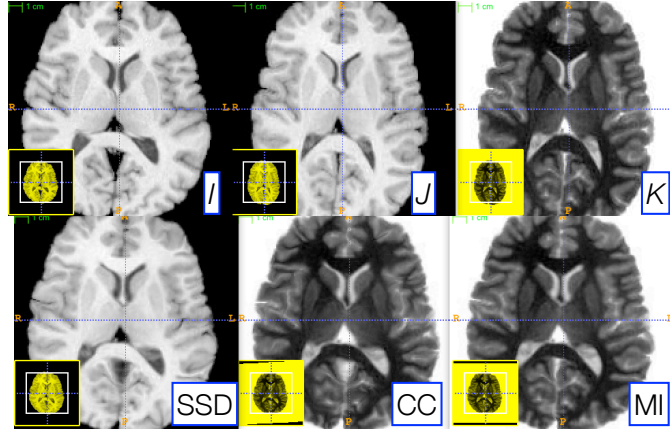
Fig. 3. Three references images, I (left), J (middle top), and K (right top), are used to illustrate the robustness of our parameter scale estimation for setting consistent parameters across both metrics and transform types. K is the negation of J and is used to test the correlation and mutual information registrations. We optimized, by hand, the step-length parameters for one metric (the sum of squared differences) for both the affine and deformable case. Thus, two parameters had to be optimized. We then applied these same parameters to register I and K via both correlation and mutual information. The resulting registrations (bottom row) were all of similar quality. Further, the same metric is used for both affine and diffeomorphic mapping by exploiting the general optimization process given in equation 1.

5 Discussion and future work

ITK is a community built and maintained toolkit and is a public resource for reproducible methods. The updated ITK[4] registration framework provides a novel set of user-friendly parameter setting tools and benchmark implementations of both standard and advanced algorithms. Robustness with respect to parameter settings has long been a goal of image registration and ITK[4] takes valuable steps toward the direction of automated parameter selection. By the time of the workshop, we intend to have a more extensive series of benchmark performance studies completed on standard datasets and hope that presentation of this work will provide a valuable foundation for future work. The number of possible applications exceeds what can possibly be evaluated via the ITK core. Community involvement is needed in order to increase the number of possible registration applications and metric / transform / optimizer / data combinations that have been evaluated. At the same time, documentation, usability and examples must be provided by the development team in order to improve user involvement. Future work will enhance the depth and breadth of this documentation as well as seek to optimize the current implementations for speed and memory. With this effort, the user community will be capable of efficiently implementing novel applications and even algorithms based on the ITK[4] framework.

References

1. Ackerman, M.J., Yoo, T.S.: The visible human data sets (VHD) and insight toolkit (ITk): experiments in open source software. AMIA Annu Symp Proc p. 773 (2003)
2. Avants, B.B., Tustison, N.J., Song, G., Cook, P.A., Klein, A., Gee, J.C.: A reproducible evaluation of ANTs similarity metric performance in brain image registration. Neuroimage 54(3), 2033–2044 (Feb 2011)
3. Baloch, S., Davatzikos, C.: Morphological appearance manifolds in computational anatomy: groupwise registration and morphological analysis. Neuroimage 45(1 Suppl), S73–S85 (Mar 2009)
4. Bearden, C.E., van Erp, T.G.M., Dutton, R.A., Tran, H., Zimmermann, L., Sun, D., Geaga, J.A., Simon, T.J., Glahn, D.C., Cannon, T.D., Emanuel, B.S., Toga, A.W., Thompson, P.M.: Mapping cortical thickness in children with 22q11.2 deletions. Cereb Cortex 17(8), 1889–1898 (Aug 2007)
5. Chen, M., Lu, W., Chen, Q., Ruchala, K.J., Olivera, G.H.: A simple fixed-point approach to invert a deformation field. Med Phys 35(1), 81–88 (Jan 2008)
6. Cheung, M.R., Krishnan, K.: Interactive deformation registration of endorectal prostate mri using itk thin plate splines. Acad Radiol 16(3), 351–357 (Mar 2009)
7. Christensen, G.E., Rabbitt, R.D., Miller, M.I.: Deformable templates using large deformation kinematics. IEEE Trans Image Process 5(10), 1435–1447 (1996)
8. Fedorov, A., Li, X., Pohl, K.M., Bouix, S., Styner, M., Addicott, M., Wyatt, C., Daunais, J.B., Wells, W.M., Kikinis, R.: Atlas-guided segmentation of vervet monkey brain MRI. Open Neuroimag J 5, 186–197 (2011)
9. Floca, R., Dickhaus, H.: A flexible registration and evaluation engine (f.r.e.e.). Comput Methods Programs Biomed 87(2), 81–92 (Aug 2007)
10. Hermosillo, G., Chefd'Hotel, C., Faugeras, O.: A variational approach to multi-modal image matching. Intl. J. Comp. Vis. 50(3), 329–343 (2002)
11. Jack, Jr, C.R., Knopman, D.S., Jagust, W.J., Shaw, L.M., Aisen, P.S., Weiner, M.W., Petersen, R.C., Trojanowski, J.Q.: Hypothetical model of dynamic biomarkers of the Alzheimer's pathological cascade. Lancet Neurol 9(1), 119–128 (Jan 2010)
12. Jenkinson, M., Smith, S.: A global optimisation method for robust affine registration of brain images. Med Image Anal 5(2), 143–156 (Jun 2001)
13. Kikinis, R., Pieper, S.: 3d slicer as a tool for interactive brain tumor segmentation. Conf Proc IEEE Eng Med Biol Soc 2011, 6982–6984 (Aug 2011)
14. Klein, S., Staring, M., Murphy, K., Viergever, M.A., Pluim, J.P.W.: elastix: a toolbox for intensity-based medical image registration. IEEE Trans Med Imaging 29(1), 196–205 (Jan 2010)
15. Metz, C.T., Klein, S., Schaap, M., van Walsum, T., Niessen, W.J.: Nonrigid registration of dynamic medical imaging data using nd + t b-splines and a groupwise optimization approach. Med Image Anal 15(2), 238–249 (Apr 2011)
16. Miller, M.I., Beg, M.F., Ceritoglu, C., Stark, C.: Increasing the power of functional maps of the medial temporal lobe by using large deformation diffeomorphic metric mapping. Proc Natl Acad Sci U S A 102(27), 9685–9690 (Jul 2005)
17. Murphy, K., van Ginneken, B., Reinhardt, J.M., Kabus, S., Ding, K., Deng, X., Cao, K., Du, K., Christensen, G.E., Garcia, V., Vercauteren, T., Ayache, N., Commowick, O., Malandain, G., Glocker, B., Paragios, N., Navab, N., Gorbunova, V., Sporring, J., de Bruijne, M., Han, X., Heinrich, M.P., Schnabel, J.A., Jenkinson, M., Lorenz, C., Modat, M., McClelland, J.R., Ourselin, S., Muenzing, S.E.A., Viergever, M.A., De Nigris, D., Collins, D.L., Arbel, T., Peroni, M., Li, R., Sharp, G.C., Schmidt-Richberg, A., Ehrhardt, J., Werner, R., Smeets, D., Loeckx, D., Song, G., Tustison, N., Avants, B., Gee, J.C., Staring, M., Klein, S., Stoel,

B.C., Urschler, M., Werlberger, M., Vandemeulebroucke, J., Rit, S., Sarrut, D., Pluim, J.P.W.: Evaluation of registration methods on thoracic ct: the empire10 challenge. IEEE Trans Med Imaging 30(11), 1901–1920 (Nov 2011)

18. Nielsen, M., Florack, L., Deriche, R.: Regularization, scale-space, and edge detection filters. J. Math. Imaging Vis. 7, 291–307 (October 1997)

19. Peyrat, J.M., Delingette, H., Sermesant, M., Xu, C., Ayache, N.: Registration of 4d cardiac ct sequences under trajectory constraints with multichannel diffeomorphic demons. IEEE Trans Med Imaging 29(7), 1351–1368 (Jul 2010)

20. Rueckert, D., Sonoda, L.I., Hayes, C., Hill, D.L., Leach, M.O., Hawkes, D.J.: Nonrigid registration using free-form deformations: application to breast mr images. IEEE Trans Med Imaging 18(8), 712–721 (Aug 1999)

21. Shelton, D., Stetten, G., Aylward, S., Ibez, L., Cois, A., Stewart, C.: Teaching medical image analysis with the insight toolkit. Med Image Anal 9(6), 605–611 (Dec 2005)

22. van Dalen, J.A., Vogel, W., Huisman, H.J., Oyen, W.J.G., Jager, G.J., Karssemeijer, N.: Accuracy of rigid CT-FDG-PET image registration of the liver. Phys Med Biol 49(23), 5393–5405 (Dec 2004)

23. Vercauteren, T., Pennec, X., Perchant, A., Ayache, N.: Diffeomorphic demons: efficient non-parametric image registration. Neuroimage 45(1 Suppl), S61–S72 (Mar 2009)

24. Yoo, T.S., Ackerman, M.J., Lorensen, W.E., Schroeder, W., Chalana, V., Aylward, S., Metaxas, D., Whitaker, R.: Engineering and algorithm design for an image processing api: a technical report on itk–the insight toolkit. Stud Health Technol Inform 85, 586–592 (2002)
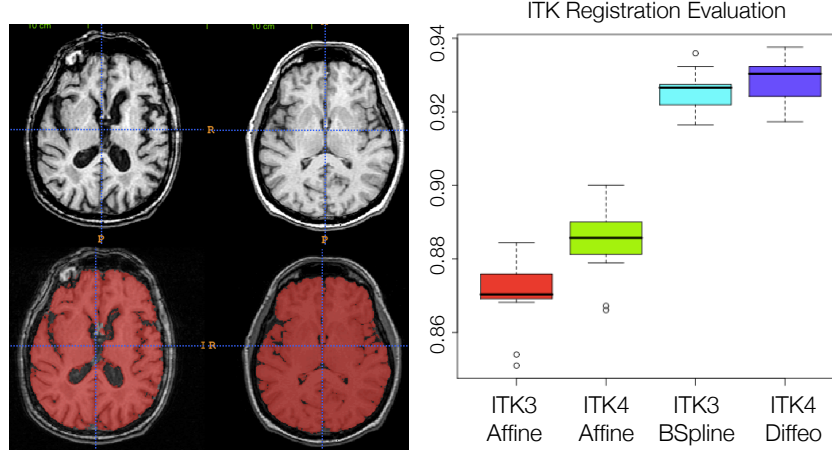
Fig. 4. We define an affine schema as $I \approx_{\mathrm{mi}} \to J_i$ for affine mapping a set of $\{J_i\}$ images to a template I. We also define a composite schema as $I \approx_{\mathrm{cc}} \leftrightsquigarrow \approx_{\mathrm{mi}} \to J_i$ for affine mapping a set of $\{J_i\}$ images to a template I. We use this schematic in a registration-based brain extraction, from MRI, in an elderly population as a benchmark for algorithm performance, similar to [14]. Example images from the dataset are at left. To gain an idea of performance variance with respect to template, we use each image in the set as template and map to all other images. In this study, there are 10 images, thus leading to a total of 45 registrations. We compare a well-used and hand optimized implementation of multi-resolution gradient descent with the previous ITK release with that of the ITK^4 framework where the ITK^4 framework uses automatically adjusted parameter scales and the v4 implementation of the mutual information metric. The metric for the v4 registration is based on that for v3. For affine registration, the average brain parcenchyma Dice overlap for the v4 framework is 0.885, while that for v3 is 0.870. The difference in performance is statistically significant (p $< 1.e - 8$), as assessed with a paired t-test. For deformable registration ITK^4 produces an average Dice of 0.929, while ITK^3 leads to Dice of 0.925. This difference is also significant at p$< 1.e - 3$.Thus, our new approach to parameter estimation—and refactoring of the framework—has allowed us to improve performance even in the basic case of whole head registration for brain extraction.